DOI:10.1021/ic802448z

Inorganic Chemistry
Article

Semiorganic Nonlinear Optical Material: Preparation and Properties of $(NH_4)\cdot Sr[L\text{-}(+)\text{-}C_4H_2O_6\cdot B(OH)_2]\cdot 4H_2O$

Xiaoyun Fan,[†,‡] Shilie Pan,[*,†] Xueling Hou,[†] Gang Liu,[§] and Jide Wang[§]

[†]*Xinjiang Technical Institute of Physics & Chemistry, Chinese Academy of Sciences, 40-1 South Beijing Road, Urumqi 830011, China,* [‡]*Graduate School of the Chinese Academy of Sciences, Beijing 100039, China, and* [§]*College of Chemistry and Chemical Engineering, Xinjiang University, Urumqi 830046, China*

Received December 25, 2008

The synthesis, crystal structure, and characterization of the noncentrosymmetric semiorganic material $(NH_4)\cdot Sr[L\text{-}(+)\text{-}C_4H_2O_6\cdot B(OH)_2]\cdot 4H_2O$ were reported. Crystals were synthesized through slow evaporation at room temperature, utilizing $SrCl_2\cdot 6H_2O$, $C_4H_4O_6$, H_3BO_3, and $NH_3\cdot H_2O$ as reagents, and its structure was determined by single-crystal X-ray diffraction. It crystallizes in the triclinic space group *P*1 (No. 1) with $a = 6.4633(10)$ Å, $b = 7.0452(13)$ Å, $c = 7.0745(12)$ Å, $\alpha = 85.351(5)°$, $\beta = 77.678(5)°$, $\gamma = 73.276(4)°$, and $Z = 1$. It exhibits a two-dimensional layered structure along the *c* axis, consisting of SrO_9 polyhedra, BO_4 tetrahedra, tartrate molecules, NH_4^+ cations, and H_2O molecules. IR spectroscopy, UV−vis diffuse-reflectance spectroscopy, thermal analysis, and second-harmonic generation (SHG) were also performed on the reported material. Nonlinear optical measurements, using 1064 nm radiation, indicate that the material has SHG properties, with an efficiency of approximately 1.5 times that of KH_2PO_4.

Introduction

In recent years, crystal structures with noncentrosymmetric (NCS) packing have attracted much attention owing to their uses in the fields of pyroelectricity, piezoelectricity, ferroelectricity, and second-order nonlinear optical (NLO) materials.[1−3] A variety of strategies have been put forth in the design of new NCS materials including the organization of molecular building blocks into a NCS crystal packing.[4,5] Among the inorganic NLO materials that have been designed, many borate systems containing alkali-metal, alkaline-earth-metal, rare-earth, and transition-metal elements resulted in the development of many important NLO crystals.[6,7] It is difficult, however, to induce acentric packing in inorganic systems.[8,9] Therefore, organic materials have been investigated because of the potential for facile modification of molecular properties through precise synthetic methods.[10,11] Compared to conventional inorganic NLO materials, organic materials have various advantages, including high optical nonlinearities and fast response times, and numerous organic NLO materials have been discovered.[12] However, organic materials also have some intrinsic weaknesses: poor physicochemical stability and low mechanical strength.[13] As a result, the investigation of semiorganic compounds as

* To whom correspondence should be addressed. E-mail: slpan@ms.xjb.ac.cn. Phone: (86)991-3674558. Fax: (86)991-3838957.

(1) Lang, S. B. *Phys. Today* **2005**, *58*, 31.
(2) Auciello, O.; Scott, J. F.; Ramesh, R. *Phys. Today* **1998**, *51*, 22.
(3) (a) Chen, C. T.; Liu, G. Z. *Annu. Rev. Mater. Sci.* **1986**, *16*, 203. (b) Becker, P. *Adv. Mater.* **1998**, *10*, 979. (c) Halasyamani, P. S.; O'Hare, D. *Chem. Mater.* **1998**, *10*, 646.
(4) Halasyamani, P. S.; Poeppelmeier, K. R. *Chem. Mater.* **1998**, *10*, 2753.
(5) Zyss, J.; Oudar, J. L. *Phys. Rev. A* **1982**, *26*, 2028.
(6) Grice, J. D.; Burns, P. C.; Hawthorne, F. C. *Can. Mineral.* **1999**, *37*, 731.
(7) (a) Chen, C. T.; Wu, B. C.; Jiang, A. D.; You, G. M. *Sci. Sin.* **1985**, *B18*, 235. (b) Chen, C. T.; Wu, Y. C.; Jiang, A.; You, G.; Li, R.; Lin, S. *J. Opt. Soc. Am.* **1989**, *B6*, 616. (c) Wu, Y. C.; Sasaki, T.; Nakai, S.; Yokotani, A.; Tang, H.; Chen, C. T. *Appl. Phys. Lett.* **1993**, *62*, 2614. (d) Sasaki, T.; Mori, Y.; Yoshimura, M. *Opt. Mater.* **2004**, *26*, 421. (e) Hagerman, M. E.; Poeppelmeier, K. R. *Chem. Mater.* **1995**, *7*, 602. (f) Mei, L. F.; Chen, C. T.; Wu, B. C. *J. Appl. Phys.* **1993**, *74*, 7014. (g) Pan, S. L.; Wu, Y. C.; Fu, P. Z.; Zhang, G. C.; Li, Z. H.; Du, C. X.; Chen, C. T. *Chem. Mater.* **2003**, *15*, 2218. (h) Pan, S. L.; Smit, J. P.; Watkins, B.; Marvel, M. R.; Stern, C. L.; Poeppelmeier, K. R. *J. Am. Soc. Chem.* **2006**, *128*, 11631.
(8) Fur, Y. L.; Beucher, M. B.; Masse, R.; Nicoud, J. F.; Levy, J. P. *Chem. Mater.* **1996**, *8*, 68.
(9) (a) Halasyamani, P. S. *Chem. Mater.* **2004**, *16*, 3586. (b) Mao, J. G.; Jiang, H. L.; Fang, K. *Inorg. Chem.* **2008**, *47*, 8498.
(10) Marder, S. R.; Beratan, D. N.; Cheng, L. T. *Science* **1991**, *252*, 103.
(11) (a) Zyss, J.; Chemla, D. S. In *Nonlinear Optical Properties of Organic Molecules and Crystals*; Nicoud, J. F., Twieg, R. J., Eds.; Academic Press: New York, 1987; Vol. 1, p 227. (b) Bosshard, Ch.; Bsch, M.; Liakatas, I.; Jger, M.; Gnter, P. In *Nonlinear Optical Effects and Materials*; Gnter, P., Ed.; Springer-Verlag: Berlin, 2000; Chapter 3.
(12) (a) Singh, S.; Bonner, W. A.; Potopowicz, J. R.; Van Uitert, L. G. *J. Appl. Phys.* **1970**, *17*, 292. (b) Xu, D.; Jiang, M.; Tan, Z. *Acta Chim. Sin.* **1983**, *41*, 570. (c) Babu, D. R.; Jayaraman, D.; Kumar, R. M.; Ravi, G.; Jayavel, R. *J. Cryst. Growth* **2003**, *250*, 157. (d) Haja-Hameed, A. S.; Anandan, P.; Jayavel, R.; Ramasamy, P.; Ravi, G. *J. Cryst. Growth* **2003**, *249*, 316. (e) Muralidharan, R.; Mohankumar, R.; Jayavel, R.; Ramasamy, P. *J. Cryst. Growth* **2003**, *259*, 321. (f) Kumar, R. M.; Babu, D. R.; Jayaraman, D.; Jayavel, R.; Kitamura, K. *J. Cryst. Growth* **2005**, *275*, e1935.
(13) (a) Jiang, M. H.; Fang, Q. *Adv. Mater.* **1999**, *2*, 1147. (b) Evans, C. C.; Bagieu-Beucher, M.; Masse, R.; Nicoud, J. F. *Chem. Mater.* **1998**, *10*, 847.

Published on Web 4/9/2009

potential NLO materials hopes to combine the advantages of the inorganic and organic systems.[14] Until now, there have been few materials that contain both the borate and tartrate groups.[15,16] An investigation of the borate−tartrate system led to the discovery of a new NLO material, $(NH_4)\cdot Sr[L\text{-}(+)\text{-}C_4H_2O_6\cdot B(OH)_2]\cdot 4H_2O$ (SCB).

The compound $(NH_4)_2O\cdot 2SrO\cdot 2C_4H_4O_5\cdot B_2O_3\cdot 10H_2O$ was first reported in 1957.[15] Zviedre et al.[16] synthesized the compound by a similar method and suggested that the formula should be $(NH_4)\cdot Sr[L\text{-}(+)\text{-}C_4H_2O_6\cdot B(OH)_2]\cdot 4H_2O$, that is, SCB. It is noteworthy that the compound has a different molecular formula in these studies.[15,16] To our knowledge, all of these investigations were focused on the synthesis of SCB and the studies of the optical properties have not been reported, particularly for the second-order NLO properties. Apart from that, the need for further understanding of the relationship between the structure and properties of SCB prompts us to reinvestigate the crystal structure of SCB using the single-crystal X-ray diffraction (XRD) technique, which permits us to establish with certainty the existence and formula of a compound. The present paper reports the synthesis, structure, and characterization of the SCB crystal.

Experimental Section

Synthesis and Growth. Polycrystalline samples of SCB were synthesized through slow evaporation. $SrCl_2\cdot 6H_2O$ (Tianjin Bodi Chemical Co., Ltd., 99.5%), tartaric acid (L-(+)-$C_4H_4O_6$; Beijing Huateng Chemical Co., Ltd., 99.5%), and H_3BO_3 (Tianjin Baishi Chemical Industry Co., Ltd., 99.5%) powders were mixed in a molar ratio of 1:1:10 and then dissolved in deionized water. The solution was thoroughly mixed under ultrasonic agitation at 50 °C for 0.5 h and then cooled down to room temperature, after which $NH_3\cdot H_2O$ (Urumqi Tianyue Chemical Reagent Co., Ltd., 27.5%) was added to the solution until the pH was above 10.5. The obtained solution was allowed to evaporate slowly at room temperature. After 2 weeks, the crystalline products were obtained and washed with excess deionized water. The experimental powder XRD (PXRD) pattern of SCB was in agreement with the one reported previously,[16] which suggested that the reported phase was recovered from the synthesis.

PXRD. PXRD was used to confirm the phase purity of each sample. PXRD was performed on an automated Bruker D8 ADVANCE X-ray diffractometer equipped with a diffracted-beam monochromatic set for Cu Kα (λ = 1.5418 Å) radiation and a nickel filter at room temperature in the angular range from 10 to 70° (2θ) with a scanning step width of 0.02° and a fixed counting time of 1 s/step.

X-ray Crystallographic Studies. A colorless and transparent crystal of SCB with dimensions 0.22 × 0.18 × 0.15 mm^3 was chosen for structure determination. Unit cell parameters were derived from a least-squares analysis of 2502 reflections in the range of $3.02° < \theta < 25.49°$. Intensity data were collected on a Rigaku R-axis Spider using graphite-monochromated Mo Kα radiation (λ = 0.710 73 Å) and integrated with the *SAINT-Plus* program.[17] All calculations were performed with the *SHELXTL-97* crystallographic software package.[18] The crystal structure was solved in space group *P*1. Final least-squares refinement on F_o^2 with data having $F_o^2 \geq 2\sigma(F_o^2)$ includes anisotropic displacement parameters for non-H atoms. The final difference Fourier synthesis may have shown maximum and minimum peaks at 1.102 and −0.960 e/Å^3, respectively.

The structure was checked for missing symmetry elements with *PLATON*.[19] Crystal data and structure refinement information are summarized in Table 1. Final atomic coordinates and equivalent isotropic displacement parameters of the title compound are listed in Table S1 in the Supporting Information. Selected interatomic distances and angles are given in Table S2 in the Supporting Information.

Table 1. Crystal Data and Structure Refinement for SCB

empirical formula	$(NH_4)\cdot Sr[L\text{-}(+)\text{-}C_4H_2O_6\cdot B(OH)_2]\cdot 4H_2O$
fw	368.61
temperature (K)	293(2)
cryst syst	triclinic
space group	*P*1 (No. 1)
unit cell dimens	a = 6.4633(10) Å; α = 85.351(5)°
	b = 7.0452(13) Å; β = 77.678(5)°
	c = 7.0745(12) Å; γ = 73.276(4)°
volume (Å^3)	301.34(9)
Z	1
density (calcd) (g/cm^3)	2.031
abs coeff (mm^{-1})	4.537
F(000)	186
cryst size (mm^3)	0.22 × 0.18 × 0.15
θ range for data collection (deg)	3.02−25.49
limiting indices	$-7 \leq h \leq 7, -8 \leq k \leq 8, -8 \leq l \leq 8$
reflns collected	2502/1888 [R(int) = 0.0484]
completeness to θ = 25.49° (%)	99.8
max and min transmn	0.5493 and 0.4352
data/restraints/param	1888/3/173
GOF on F^2	1.060
final R indices [$I > 2\sigma(I)$][a]	R1 = 0.0398, wR2 = 0.0975
R indices (all data)	R1 = 0.0402, wR2 = 0.0976
extinction coeff	0.057(13)
largest diff peak and hole (e/Å^3)	1.102 and −0.960

[a] $R1 = \sum||F_o| - |F_c||/\sum|F_o|$ and $wR2 = [\sum w(F_o^2 - F_c^2)^2/\sum wF_o^4]^{1/2}$ for $F_o^2 > 2\sigma(F_o^2)$.

IR Spectroscopy. IR absorption spectroscopy of the compound was recorded on a Bruker EQUINOX 55 Fourier transform infrared spectrometer. The sample was mixed thoroughly with dried KBr (5 mg of the sample and 500 mg of KBr), and the spectrum was collected in a range from 400 to 4000 cm^{-1} with a resolution of 2 cm^{-1}.

Thermal Analysis. The thermal analyses for SCB were carried out on a simultaneous thermal analyzer, a Netzsch STA 449C instrument, with a heating rate of 10 °C/min in an atmosphere of flowing air from 25 to 900 °C. A ceramic (Al_2O_3) crucible was used for heating.

Elemental Analysis. The elemental analyses (C, H, and N) were determined on a PE-2400 element analyzer. A summary of the inductively coupled plasma elemental analysis of Sr and B was performed using a Varian Vita-Pro CCD simultaneous inductively coupled plasma−optical emission spectroscopy spectrometer. Anal. Calcd for SCB: C, 13.03; H, 4.38; N, 3.80; Sr, 23.77; B, 2.93. Found: C, 13.01; H, 4.37; N, 3.82; Sr, 23.77; B, 2.93.

UV−Vis Diffuse-Reflectance Spectroscopy. UV−vis diffuse-reflectance data for SCB crystalline samples were collected with a TU-1901 UV−vis−near-IR spectrophotometer with $BaSO_4$ as the standard, which has a cutoff point at about

(14) (a) Kanis, D. R.; Lacroix, P. G.; Ratner, M. A.; Marks, T. J. *J. Am. Chem. Soc.* **1994**, *116*, 10089. (b) Jiang, M. H.; Xu, D.; Xing, G. C.; Shao, Z. S. *J. Syn. Cryst.* (*in Chinese*) **1985**, *14*, 1. (c) Xu, D.; Jiang, M. H.; Tan, Z. G. *Acta. Chim. Sin.* **1983**, *41*, 570.
(15) Shvarts, E. M.; Ievin'sh, A. F. *J. Inorg. Chem. USSR* **1957**, *2*, 1757.
(16) Zviedre, J.; Belsky, V.; Schwartz, J. *J. Inorg. Chem.* (*in Latvian*) **1999**, *3*, 3.
(17) *SAINT-Plus*, version 6.02A; Bruker Analytical X-ray Instruments, Inc.: Madison, WI, 2000.
(18) Sheldrick, G. M. *SHELXTL*, version 6.14; Bruker Analytical X-ray Instruments, Inc.: Madison, WI, 2003.
(19) Spek, A. L. *J. Appl. Crystallogr.* **2003**, *36*, 7.

240 nm. Reflectance spectra were converted to absorbance with the Kubelka−Munk function.[20,21] The spectrum of SCB is shown in Figure S3 in the Supporting Information.

NLO Measurements. Powder second-harmonic generation (SHG) tests were carried out on SCB by the Kurtz−Perry method.[22] Microcrystalline KDP served as the standard. About 100 mg of powder was pressed into a pellet, which was then irradiated with a pulsed IR beam (10 ns and 10 kHz) produced by a Q-switched Nd:YAG laser of wavelength 1064 nm. A 532 nm filter was used to absorb the fundamental and pass the visible light onto a photomultiplier. A combination of a half-wave achromatic retarder and a polarizer was used to control the intensity of the incident power, which was measured with an identical photomultiplier connected to the same high-voltage source. This procedure was then repeated using a standard NLO material, in this case microcrystalline KDP, and the ratio of the second-harmonic intensity outputs was calculated. Because the SHG efficiency has been shown to depend strongly on the particle size,[23] polycrystalline SCB was ground and sieved into distinct particle size ranges, <20, 20−38, 38−55, 55−88, 88−105, 105−150, and 150−200 μm. To make relevant comparisons with known SHG materials, crystalline SiO_2 and KDP samples were also ground and sieved into the same particle size ranges.

Results and Discussion

Synthesis. During synthesis of the compound, a variety of reaction conditions were attempted, with pH values ranging from 7 to 12 and several different reaction temperatures. The results show that temperature is not the main factor for formation of the compound, whereas the pH value is critical for crystal growth. It is difficult to obtain the desired crystal when the pH is below 10 (detailed results are shown in Table S3 in the Supporting Information). As shown, when a pH value of around 10.5 was selected, it took less than 1 week to obtain the SCB crystal. The sample purity was verified using XRD, shown in Figure S1 in the Supporting Information. The experimental PXRD pattern of SCB is in agreement with the calculated XRD pattern based on the single-crystal data, suggesting that the synthesized phase is pure (see Figure S2a in the Supporting Information). Additionally, the other "hand" was also synthesized by using D-(−)-tartaric acid, and its PXRD pattern is the same as the one synthesized by using L-(+)-tartaric acid, shown in Figure S2b in the Supporting Information.

Crystal Structure. The SCB structure exhibits a two-dimensional layered structure along the *c* axis, consisting of SrO_9 polyhedra, BO_4 tetrahedra, tartrate molecules, NH_4^+ cations, and H_2O molecules (see Figure 1). The structural layers in the crystal structure are connected by hydrogen bonds involving NH_4^+ cations and H_2O molecules (see Figure 2).[24] The Sr−O distances range from 2.581(5) to 2.793(6) Å, and the average distance Sr−O is 2.687(6) Å, which is similar to other results reported,[25] with the O−Sr−O angles ranging from 52.66(14)° to 157.43(17)°. Each B atom is bonded to four O atoms (see Figure S2b in the Supporting Information). B−O distances range from 1.447(11) to 1.498(10) Å, and the mean distance for B−O bonds is 1.469 Å, with O−B−O angles ranging from 105.9(6)° to 124.0(7)°. Owing to a twist of the carbon chain in the tartaric acid molecule, the tartaric acid molecule is not coplanar, with the torsion angle for the four carbons in the tartrate 147.220° (see Figure 3).

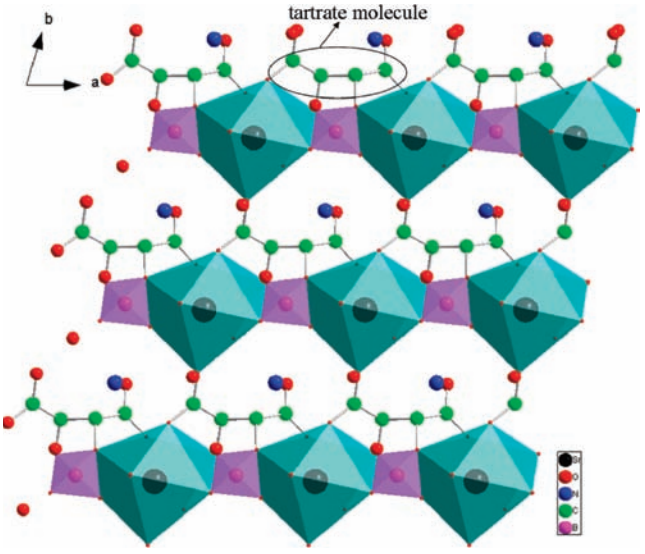

Figure 1. Fundamental building unit of SCB. View of the structure of SCB along the *c* axis. The H atoms have been removed for clarity. SrO_9 polyhedra are shown in aqua, BO_4 tetrahedra are shown in pink, and one of the tartrate molecules is labeled by a circle.

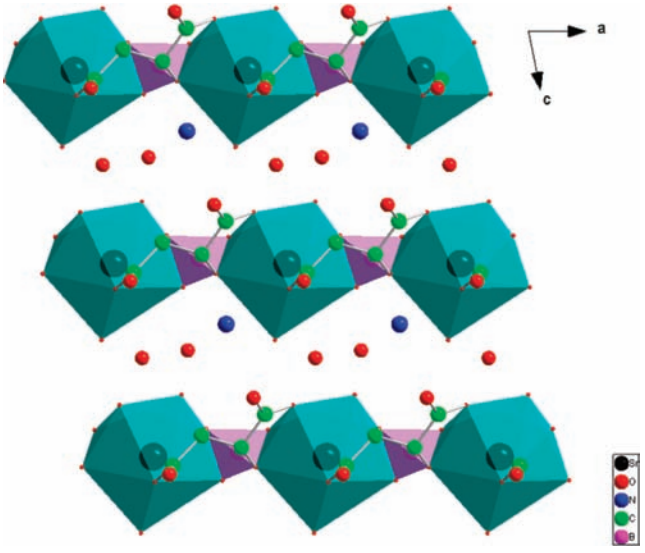

Figure 2. Fundamental building unit of SCB. View of the structure of SCB along the *b* axis. The H atoms have been removed for clarity. The NH_4^+ cations and H_2O molecules interact with the layers through N−H—O and O−H—O hydrogen bonding.

From XRD, it is difficult to tell the differences among N, O, and C atoms. If nitrogen is placed at the oxygen position, it will not affect the refinement results. In order to determine whether nitrogen exists in the molecule, the compound was further characterized by IR spectroscopy and element analysis.

IR Spectroscopy. As indicated in Figure S4 in the Supporting Information, the characteristic peaks of SCB can be described as follows: Between 1000 and 820 cm^{-1}, we observe the absorption peaks typical for

(20) Tauc, J. *Mater. Res. Bull.* **1970**, *5*, 721.
(21) Kubelka, P.; Munk, F. *Tech. Phys.* **1931**, *12*, 593.
(22) Kurtz, S. Q.; Perry, T. T. *J. Appl. Phys.* **1968**, *39*, 3798.
(23) Dougherty, J. P.; Kurtz, S. K. *J. Appl. Crystallogr.* **1976**, *9*, 145.
(24) Kim, J. H.; Baek, J.; Halasyamani, P. S. *Chem. Mater.* **2007**, *19*, 5637.
(25) Wu, L.; Zhang, Y.; Chen, X. L.; Kong, Y. F.; Sun, T. Q.; Xu, J. J.; Xu, Y. P. *J. Solid State Chem.* **2007**, *180*, 1470.

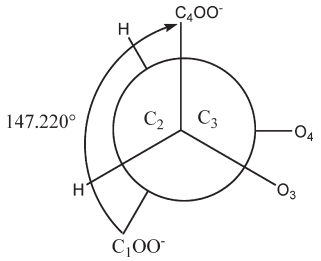

Figure 3. Torsion angles for L-(+)-tartaric acid by Newman projection.

BO_4 groups as in $MgAlBO_4$, $Ca[B(OH)_4]_2$, and SrB_4O_7, and peaks at 959 and 898 cm^{-1} can be attributed to asymmetric stretching and symmetric stretching vibrations of B−O, respectively.[26] The deformation vibration at 674 cm^{-1} can be assigned as the in-plane stretching vibration of B−O, and 509 cm^{-1} is the out-of-plane stretching vibration. At 1111 cm^{-1}, the stretching vibration of C−O is observed, and at 1600 cm^{-1}, the stretching vibration of C=O appears.[27] The bands at 1414 cm^{-1} can be assigned to the distortion vibration of NH_4^+,[28] and the bands at 3492 and 3229 cm^{-1} are the O−H and N−H stretching vibration modes of the strong hydrogen bonds, respectively.

Thermal Analysis. The results of the thermal analyses are represented by the curves in Figure 4. From the thermogravimetric analysis (TGA) curve, it can be seen that weight loss occurs in four stages: It is obvious that the material is very stable, and there is no weight loss when the temperature is lower than 100 °C. Then, it undergoes a weight loss between 100 and 150 °C because of the release of the four molecules of H_2O, which corresponds to a relative weight loss of 19%. Between 150 and 220 °C, the loss of a NH_4^+ anion is shown, approximately equal to a 4% weight loss. Between 220 and 690 °C, the curve indicates a complete loss of water and decomposition of the tartrate. PXRD measurements, after this step, revealed that the materials are mainly SrB_2O_4 and partial SrB_4O_7, which accounts for a total weight of 55.8%. In the fourth stage, occurring between 690 and 900 °C, weight loss might be attributed to the gradual volatilization of boron oxide from SrB_4O_7.[29] PXRD measurements revealed that the final residues mainly are SrB_2O_4 and partial SrO (see Figure S5 in the Supporting Information), which accounted for a total weight of 42.5%. The differential thermal analysis (DTA) curve of SCB is consistent with the above deductions. The sharp endothermic peak at 144 °C is due to the loss of four H_2O molecules. The sharp exothermic peaks observed at 439 and 751.5 °C could be attributed to combustion of the organic unit and the phase transition of the residual oxides, respectively.

These results are in accordance with the compositions of the compounds determined by elemental analyses.

Elemental Analysis. The stoichiometry was calculated on the basis of one Sr atom and one B atom in each formula unit. From the organic elemental analysis of the title compound, the molecule indeed contains nitrogen.

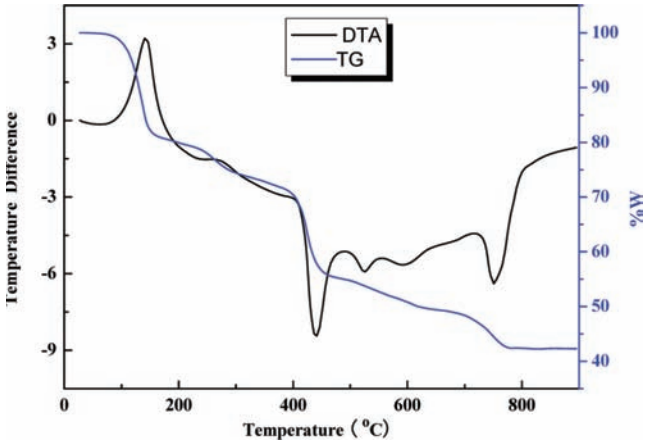

Figure 4. TGA/DTA curve of the SCB crystal.

UV−Vis Diffuse-Reflectance Spectroscopy. The UV−vis diffuse-reflectance spectrum for SCB is deposited in Figure S6 in the Supporting Information. The compound is colorless, and the spectra indicate that it is transparent. Between 250 and 900 nm, the transmission is above 85%. Absorption (K/S) data were calculated from the following Kubelka−Munk function:

$$F(R) = \frac{(1-R)^2}{2R} = \frac{K}{S}$$

with R representing the reflectance, K the absorption, and S the scattering. In a K/S vs E (eV) plot, extrapolating the linear part of the rising curve to zero provides the onset of absorption at 5.49 eV. It is likely that the visible absorption in the reported compounds can be attributed to the electron transfer in the tartrate molecule and partly from the B−O tetrahedra.

NLO Measurements. The compound crystallizes in a NCS space group, which is the basic condition for a potential harmonic generation material. According to the literature reported,[4] the nonlinearity of a borate crystal originates from the boron−oxygen groups, and borates containing BO_4 groups often possess a SHG effect much smaller than that of borates containing BO_3 groups. In the current experiment, green light was observed and its intensity was about as large as that of KDP when the grown crystal was ground into powder and loaded into a quartz cell. Therefore, the powder NLO effect of the compound is about the same as that of KDP. Because BO_4 tetrahedra are considered weak SHG originators, the NLO effect in SCB likely originates from tartrate groups. Furthermore, Nicoud et al. have suggested[30] that organic groups grafted on an inorganic framework are always associated with a NCS crystal structure. Additionally, the presence of delocalized π-electron systems, which enhance asymmetric polarizability, is the primary reason for the nonlinearity in organic materials,[31] and such measurements also help to confirm

(26) Pascuta, P.; Pop, L.; Rada, S.; Bosca, M.; Culea, E. *J. Mater. Sci.: Mater. Electron.* **2008**, *19*, 424.
(27) (a) Finn, M. G.; Sharpless, K. B. *J. Am. Chem. Soc.* **1991**, *113*, 113. (b) Bou, J. J.; Rodriguez-Galan, A.; Munoz-Guerra, S. *Macromolecules* **1993**, *26*, 5664.
(28) Miller, F. A.; Wilkins, C. H. *Anal. Chem.* **1952**, *24*, 1253.
(29) Liu, Z. H.; Li, L. Q.; Wang, M. Z. *J. Alloys Compd.* **2006**, *407*, 334.
(30) Le Fur, Y.; Bagieu-Beucher, M.; Masse, R.; Nicoud, J. F.; Levy, J. P. *Chem. Mater.* **1996**, *8*, 68.
(31) Newman, I.; Warren, P. K.; Gumingham, L. F.; Chang, P.; Copper, T. Y.; Burdge, D. E.; Polol, L.; Lowe, D. P. *Mater. Res. Soc. Symp. Proc.* **1990**, *173*, 557.

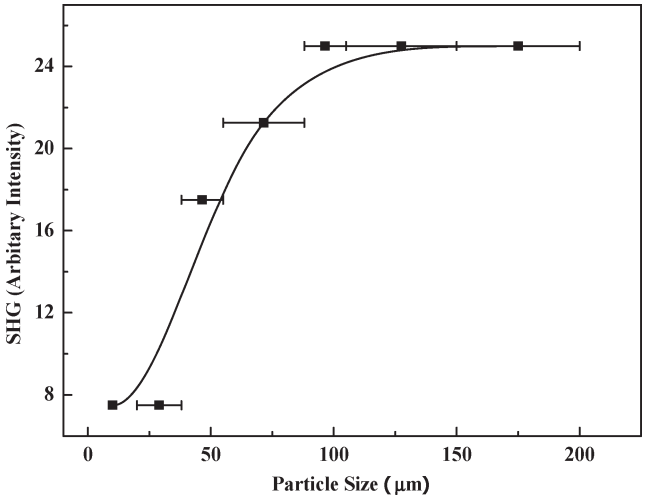

Figure 5. Phase-matching curve, that is, particle size vs SHG intensity, for SCB. The curve drawn is a guide to the eye and is not a fit to the data.

the assignment of this structure in a NCS setting. Therefore, it is considered that the main source of nonlinearity in SCB originates from tartrate groups with a very limited contribution from BO_4 groups. The SHG measurements on sieved SCB indicate that the material is phase-matchable (type I) (see Figures 5 and S7 in the Supporting Information) with an intensity of approximately 1.5 times that of KDP.

Conclusion

In summary, one novel borate−tartrate hybrid compound, $(NH_4)\cdot Sr[L\text{-}(+)\text{-}C_4H_2O_6\cdot B(OH)_2]\cdot 4H_2O$, with a NCS crystal structure has been prepared and characterized. It exhibits SHG efficiency of about 1.5 times that of KDP and is phase-matchable. Results of our studies indicate that by the introduction of an organic molecule, such as tartrate, in the borate system we can design new types of second-order NLO materials. If the above two types of units are properly aligned, it is expected that new NCS compounds with enhanced SHG response can be obtained. Our future research efforts will be devoted to the exploration of new SHG compounds by the introduction of other types of organic molecules into borates.

Acknowledgment. The authors thank Dr. Jared P. Smit for his valuable revisons. This work is supported by the National Natural Science Foundation of China (Grant 50802110), the One hundred Talents Project Foundation Program, the Western Light Joint Scholar Foundation Program of Chinese Academy of Sciences, the Natural Science Foundation of Xinjiang Uygur Autonomous Region of China (Grant 200821159), and the High Technology Research and Development Program of Xinjiang Uygur Autonomous Region of China (Grant 200816120).

Supporting Information Available: Calculated and observed PXRD patterns of the SCB compounds, IR and UV−vis transmittance spectra, and an X-ray crystallographic file in CIF format including crystallographic details and interatomic distances and angles for SCB. This material is available free of charge via the Internet at http://pubs.acs.org.